Available online at www.sciencedirect.com
SCIENCE DIRECT®
Biochemical and Biophysical Research Communications 338 (2005) 491–498
BBRC
www.elsevier.com/locate/ybbrc

The interaction domain of the redox protein adrenodoxin is mandatory for binding of the electron acceptor CYP11A1, but is not required for binding of the electron donor adrenodoxin reductase ☆

Achim Heinz [a], Frank Hannemann [a], Jürgen J. Müller [b], Udo Heinemann [b], Rita Bernhardt [a,*]

[a] *FR 8.3—Biochemie, Universität des Saarlandes, D-66041 Saarbrucken, Germany*
[b] *FG Kristallographie, Max-Delbrück-Center, Robert-Rössle-Str.10, D-13125 Berlin, Germany*

Received 25 July 2005
Available online 22 August 2005

Abstract

Adrenodoxin (Adx) is a [2Fe–2S] ferredoxin involved in electron transfer reactions in the steroid hormone biosynthesis of mammals. In this study, we deleted the sequence coding for the complete interaction domain in the Adx cDNA. The expressed recombinant protein consists of the amino acids 1–60, followed by the residues 89–128, and represents only the core domain of Adx (Adx-cd) but still incorporates the [2Fe–2S] cluster. Adx-cd accepts electrons from its natural redox partner, adrenodoxin reductase (AdR), and forms an individual complex with this NADPH-dependent flavoprotein. In contrast, formation of a complex with the natural electron acceptor, CYP11A1, as well as electron transfer to this steroid hydroxylase is prevented. By an electrostatic and van der Waals energy minimization procedure, complexes between AdR and Adx-cd have been proposed which have binding areas different from the native complex. Electron transport remains possible, despite longer electron transfer pathways.

Keywords: Adrenodoxin; Electron transfer; Ferredoxin-NADP$^+$ reductase; Protein–protein interaction; Electrostatic potential; CYP11A1

In mammals, the adrenal cortex is the primary site of synthesis of a number of important steroid hormones. Also here, oxygenases play an important role, which were discovered by Osamu Hayaishi 50 years ago as enzymes that catalyse the oxidative cleavage of substrates by incorporation of atmospheric dioxygen into the substrate. Therefore this publication is dedicated to him and his pioneering discovery. The presence of different oxygenases (i.e., cytochrome P450s), localized in either the mitochondria or endoplasmic reticulum, work in concert for the sequential oxygenation of the steroid nucleus. The initial and rate-limiting step of this biosynthesis, the conversion of cholesterol to yield pregnenolone, the precursor of all steroid hormones, is performed by the mitochondrial cholesterol converting P450 system composed of the NADPH-dependent FAD-containing adrenodoxin reductase (AdR),[1] adrenodoxin (Adx), and the cytochrome P450$_{scc}$ (CYP11A1).

Bovine Adx, localized in the mitochondrial matrix, serves as an electron transfer protein in this P450 system and also directs electrons to the cytochrome CYP11B1 involved in producing the steroid hormones cortisol and aldosterone [1]. The mature soluble form of adrenodoxin consists of 128 amino acids and belongs to the group of ferredoxins carrying a [2Fe–2S] cluster. The Adx molecule is organized in two structural domains, a core domain containing the

☆ This work was supported by grants from the Deutsche Forschungsgemeinschaft (Be1343/8-2 and He1318/19-3,4) and the Fonds der Chemischen Industrie to R.B. and U.H.
* Corresponding author. Fax: +49 681 302 4739.
E-mail address: ritabern@mx.uni-saarland.de (R. Bernhardt).

[1] *Abbreviations:* Adx, bovine adrenodoxin wild type; Adx-cd, deletion mutant of adrenodoxin lacking amino acids 60–88; AdR, adrenodoxin reductase; CYP11A1, cytochrome P450$_{scc}$; CD, circular dichroism; ET, electron transfer; SOE-PCR, site overlapping PCR; PCR, polymerase chain reaction; EDC, *N*-ethyl-*N*′-dimethylaminopropyl-carbodiimide; NHS, *N*-hydroxysuccinimide.

0006-291X/$ - see front matter © 2005 Elsevier Inc. All rights reserved.
doi:10.1016/j.bbrc.2005.08.077

iron–sulfur cluster, coordinated with four cysteines [2], and a hairpin domain [3]. The hairpin, also referred to as the recognition domain, is required for recognition and interaction of Adx with its redox partners. This recognition is mainly based on electrostatic interactions of negatively charged amino acids on the surface of Adx with positively charged amino acids of AdR or of cytochrome P450, respectively [4,5]. The different acidic residues of the recognition domain contribute unequally to the stabilization of the two complexes, but show a significant overlap for the binding site of AdR and CYP11A1 [6]. Amino acids 68–86 of Adx were shown to interact with both, AdR and CYP11A1 [7]. Aspartates 76 and 79 seem to be essential for interaction with AdR and CYP11A1, while aspartate 72 and glutamate 73 seem to interact only with CYP11A1 [8]. Tyrosine 82 has also been suggested to be close to the binding site of AdR and CYP11A1 [9]. Additional interaction sites localized in the core domain have been identified by the resolved crystal structure of a cross-linked 1:1 complex of Adx and AdR [5] as well as by site-directed mutagenesis studies. These interaction sites are localized in a second acidic patch around position Asp-39, the putative electron transfer region around the iron–sulfur cluster loop [10,11], and involve C-terminal residues of the ferredoxin [12].

Apart from the interacting residues of the redox partners, the overall organization of the functional electron transferring complex is still under investigation. Kido and Kimura [13] have reported that in the presence of cholesterol a stable 1:1:1 complex of Adx with its redox partners was formed. In contrast, Lambeth et al. [14] have proposed that Adx functions as a mobile electron shuttle transferring electrons from AdR to the cytochrome P450. According to a third model proposed by Hara and Takeshima [15], electron transfer occurs using two molecules of Adx transferring the electrons needed to the cytochrome P450. Additional evidence that Adx forms dimers has been obtained recently [16,17]. Nevertheless, how the reducing equivalent is transferred from AdR to CYP11A1 by Adx is still a matter of controversial discussion.

In this study, we describe a deletion mutant, Adx-cd, consisting of only the core domain, generated by SOE-PCR cloning. In order to investigate the specific role of the remaining interaction sites in the adrenodoxin core domain for its redox partners, the deletion mutant Adx-cd was characterized in comparison with full-length Adx by biophysical and biochemical methods. In particular, Adx-cd was analyzed in vitro for its ability to associate with AdR and with CYP11A1, for its function as electron acceptor for AdR, and for its function to support the P450-catalyzed cholesterol side-chain cleavage. The experimental results have been complemented by protein–protein docking calculations.

Materials and methods

Reagents and biochemicals. Taq DNA polymerase was from Biozym and restriction endonucleases were from GE Healthcare. Steroids were purchased from Sigma. All other reagents were of the highest purity grade commercially available.

Construction of the cDNA for adrenodoxin mutant. The cDNA of the deletion mutant Adx-cd was obtained in two subsequent reactions. In a first amplification step, two fragments with overlapping ends were produced by PCR. Fragment 1, obtained using primer pair 1 (Table 1), codes for amino acids 4–60 in wild-type adrenodoxin and continues with amino acids 89–94, which serve as the overlapping region. Fragment 2, which codes for amino acids 89–128 with an overlapping region from amino acid 55 to 60 in the N-terminal position, was produced using the primer pair 2. Together, these two fragments serve as the template for the following PCR using the forward primer from primer pair 1 and the reverse primer from primer pair 2 as a new primer pair. In this second amplification step, a fragment was obtained which codes for the mutant adrenodoxin protein. The fragment was cloned into the expression vector *pET3d* [18]. The accurate cDNA sequence was verified by sequencing.

Expression and purification. Escherichia coli strain BL21(DE3) was used for protein expression. Recombinant Adx and AdR were purified as described [2,19]. Protein concentration was calculated using $\varepsilon_{414} = 9.8$ $(\text{mM cm})^{-1}$ for Adx [20], and $\varepsilon_{450} = 11.3$ $(\text{mM cm})^{-1}$ for AdR [21]. CYP11A1 from bovine adrenal glands was isolated according to Akhrem et al. [22]. Adx-cd was purified using standard protocols for Adx isolation.

Spectroscopic methods. Absorption spectra in the UV/visible region were recorded at room temperature using a Shimadzu double-beam spectrophotometer UV2101PC.

CD spectra were recorded as described [23] using a Jasco 715 spectropolarimeter. Temperature-dependent measurements were carried out at a heating rate of 50 °C h^{-1} from 20 to 65 °C with a temperature increment of 0.2 °C, monitoring the decrease of the circular dichroism signal at 440 nm. T_m was calculated from CD scans with a nonlinear regression program using a two-state model [24,25].

EPR spectroscopy. Two hundred microliters of a 1 mM adrenodoxin solution was reduced with dithionite under anaerobic conditions in a glove box. After transferring the sample into an EPR tube, it was frozen in liquid nitrogen. EPR spectra were recorded with a Bruker spectrometer ER 420 with a microwave frequency of 9.5 GHz and a field modulation frequency of 100 kHz. An immersion Dewar flask was used for the measurements at liquid nitrogen temperature (77 K).

Redox potential measurements. Redox potentials of Adx and Adx-cd were determined using the dye photoreduction method with Safranin T as indicator and mediator as described [26].

Table 1
Oligonucleotides for SOE-PCR

	Oligonucleotide
Primer pair 1	
Forward	5′-gggg**CCATgg**gCAgCTCAgAAgATAAAATAACAgTC-3′
Reverse	5′-gATCTggCAgCCCAACCgTTCAAAgATgAggTgACA-3′
Primer pair 2	
Forward	5′-TgTCACCTCATCTTTgAAgCCTTgggCTgCCAgATC-3′
Reverse	5′-gggg**ggATCC**TTAAggTACTCgAACAgTCATATTg-3′

The sequences which code for the overlapping region are underlined and restriction sites for cloning are in bold letters. The polymerase chain reaction primers with appropriate cloning sites and overlapping sites were chemically synthesized by BioTez GmbH, Berlin.

Enzyme activity assays. The interaction of Adx and AdR was assayed following the reduction of cytochrome *c* in a buffer containing 20 mM potassium phosphate (pH 7.4) and 10 mM potassium chloride. The reaction was initiated by the addition of NADPH. The absorption change at 550 nm was monitored, and the activity was determined using an extinction coefficient of 20 mM cm^{-1} for cytochrome *c*. Additionally, the electron transfer from AdR to Adx was also assayed following the reduction of Adx in a buffer containing 20 mM potassium phosphate, pH 7.4. The reaction was initiated by the addition of NADPH. The absorption change at 415 nm was monitored.

The cholesterol side-chain cleavage was assayed in a reconstituted system catalyzing the conversion of cholesterol to pregnenolone according to the procedure of Sugano et al. [27]. Assays were performed at 30 °C in 50 mM potassium phosphate, pH 7.4, 0.1% Tween 20 and contained a NADPH regenerating system. The samples were analyzed by reversed-phase HPLC with an isocratic system of acetonitril/isopropanol (30:1).

Optical biosensor measurements. The interaction between Adx and AdR, as well as the interaction between Adx and CYP11A1, was assayed using a BIAcore X system and CM5 chips, i.e., a carboxy-methylated dextran surface for coupling of adrenodoxin. Adx was immobilized onto the sensor surface using a mixture of EDC and NHS (Biacore, Uppsala, Sweden) with a flow rate of 5 µl min^{-1} at 20 °C. The sensor surface was activated using two injections of 50 µl of a mixture of EDC and NHS. A continuous flow of HBS-EP buffer (10 mM Hepes buffer, pH 7.4 containing 0.15 M NaCl, 3 mM EDTA, and 0.005% (v/v) polysorbate 20) was maintained over the sensor surface. Specific surfaces were obtained by injecting Adx or Adx-cd. These proteins were diluted in HBS-EP and used at a concentration of 60 µM. The procedure of immobilizing the protein was completed by an injection of 50 µl with a flow rate of 10 µl min^{-1} 1 M ethanolamine hydrochloride to block the remaining ester groups. Eight hundred response units (RU) of both proteins was immobilized, which corresponds to 0.8 ng protein mm^{-2} sensor surface. The Adx/AdR interaction was investigated by applying AdR solutions ranging from 10 nM to 2 µM diluted in HBS with a continuous flow of 10 µl min^{-1}. Before each measurement, the Adx-surface was regenerated with 2 mM NaOH. The same was performed using CYP11A1 as a second interaction partner of Adx.

Docking experiments. Crystal structures of AdR and Adx have been determined recently [3,5]. A three-dimensional structure of the Adx-cd was then calculated by the Swiss-Model [28]. Because intermolecular interactions involving Adx-cd are electrostatically driven in the same way as Adx-ligand binding, theoretical docking of Adx-cd to AdR was performed using the calculation of minimum electrostatic and van der Waals energy of a complex between both. We followed the strategy described recently by Müller et al. [29] using the program DOT [30]. AdR was fixed in the center of a 1-Å spaced grid and Adx-cd was moved from grid point to grid point around AdR. At each grid point, the moving molecule was rotated with a 6° sampling searching for the minimum energy of the complex. The shape of the moving molecule was approximated by its atomic coordinates not taking into account the van der Waals volumina [30] of the atoms to permit an approach within 1.5 Å of the stationary molecule and small side-chain conformational changes upon docking. The partial charges were taken from the AMBER library [31] and placed at the atomic positions of the non-hydrogen and polar hydrogen atoms. The shape of the stationary molecule was defined by a 3.0-Å layer of favorable potential. To avoid large changes in magnitude and distribution of the electrostatic potential, extremes of >4 and <−6 kcal mol^{-1} e^{-1} were cancelled [29]. In the minimum-energy search by DOT, $128 \times 128 \times 128$ grid points and 54,000 rotational orientations were used. The calculation took 50 h on four SGI octanes with 400-MHz processors.

Results

Protein expression and purification

Adx-cd was expressed as a holoprotein with a yield of 1100 nmol L^{-1} of *E. coli* culture. The protein was purified to homogeneity, yielding a *Q*-value (A_{415}/A_{276}) of 0.5. Adx-cd has a calculated molecular weight of 10.7 kDa.

Spectral characterisation of Adx-cd

Adx-cd exhibits absorption spectra characteristic of a correctly assembled [2Fe–2S] cluster (Fig. 1A). Slight differences can be found in the UV/Vis spectra of oxidized and reduced Adx-cd (data not shown) compared with Adx, such as a higher absorption at 458 nm in the oxidized state and a slight drift of the maximum from 415 to 413 nm.

Circular dichroism (CD) spectra of the adrenodoxin mutant show changes in the absorbance maximum, which is usually at 440 nm for the wild type. A drift of 2 nm from 440 to 438 nm could be detected for Adx-cd. In addition, the shape of the peak at 438 nm changed in comparison to the Adx signal at 440 nm (Fig. 1B). This unsymmetric peak indicates changes in the environment of the iron–sulfur cluster. Furthermore, in the aromatic region (near-UV region) of the CD spectra, changes could be observed and a slight effect could also be observed in the far-UV region, which might be due to local conformational changes of the mutant.

EPR spectra of Adx-cd (Fig. 1C) displayed a slight modification in the $g_{\perp}$ as compared with Adx spectra. Additionally, a second signal of 1927 was obtained which indicates slight changes in the conformation of the iron–sulfur cluster. A $g_{\parallel}$ value of 2.02 was measured for both Adx as well as the mutant protein Adx-cd.

Redox potential

Although the molecular parameters determining the redox potential of a protein are not fully understood, changes in the redox potential of ferredoxins seem to reflect either changes in the nature of the ligands or in the water accessibility of the metal clusters, e.g., conformational changes of the cluster environment. The redox potential of Adx-cd was estimated to be -282 ± 5 mV under our experimental condition which is about 8 mV lower compared with Adx. This is in agreement with the spectroscopic data which also indicate small changes in the cluster environment.

Thermal stability

Thermal unfolding of Adx and Adx-cd upon increasing temperature was followed by measuring their circular dichroism. Single-wavelength melting curves were recorded at 440 nm, where the maximal circular dichroism of the iron–sulfur cluster is observed by slowly increasing the temperature from 20 to 65 °C. The circular dichroism signal decreases in a sigmoidal manner upon increasing temperature, allowing a corresponding fit of the data. With 48.7 °C, the T_m value of the oxidized Adx-cd is only 0.8 °C lower than that of wild-type Adx (Fig. 1D), and reduced proteins also show similar results. Measurements

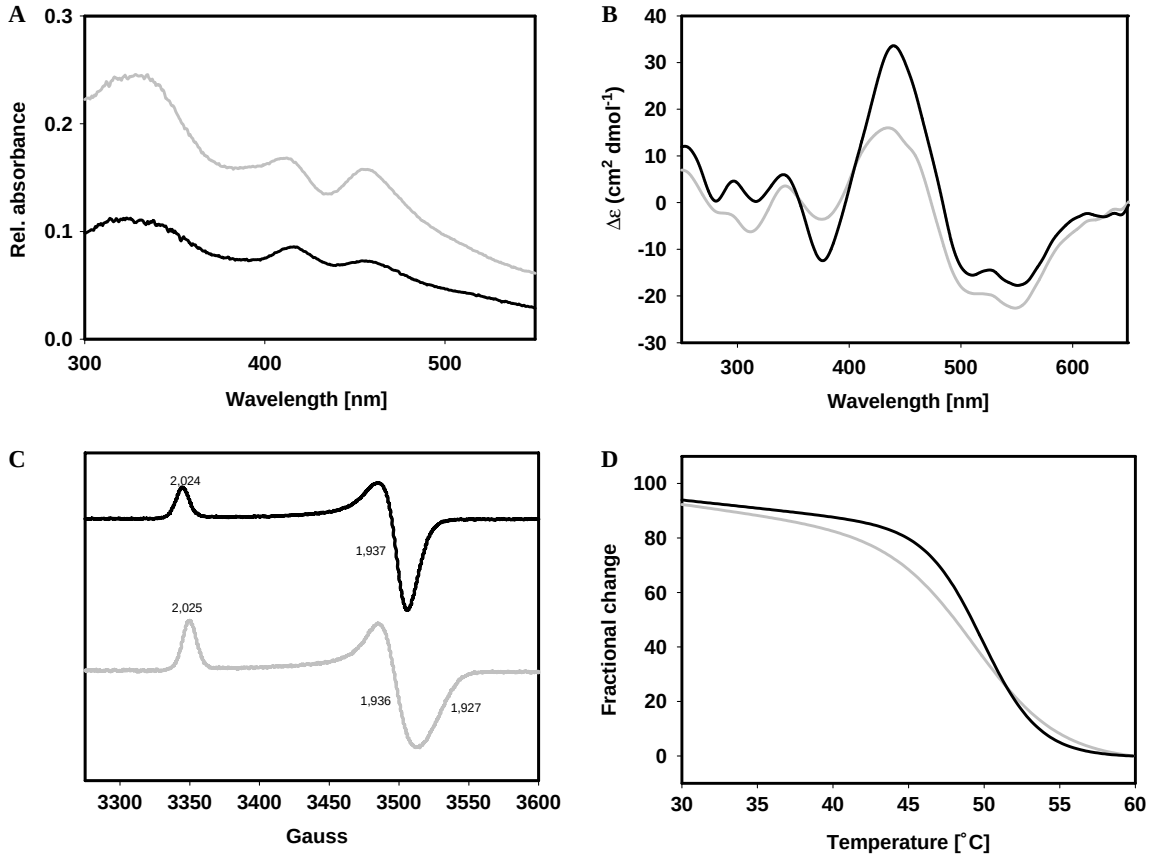

Fig. 1. Spectroscopical analysis of Adx and Adx-cd. (A) The absorbance spectra of Adx (black) and Adx-cd (gray) were measured using a Shimadzu double-beam spectrophotometer UV2101PC. The concentration of the proteins was 1 mM in 10 mM potassium phosphate buffer (pH 7.4). (B) Samples used for CD spectra in the visible range of Adx (black) and Adx-cd (gray) contained 100 μM adrenodoxin in 10 mM potassium phosphate buffer (pH 7.4). (C) EPR spectra of 1 mM reduced recombinant samples (black—Adx, grey—Adx-cd) were taken at 77 K in 10 mM potassium phosphate buffer, pH 7.4. (D) Single-wavelength melting curves were recorded at 440 nm for Adx (black) and Adx-cd (gray). The temperature of 40 μM adrenodoxin solutions was slowly increased from 20 to 65 °C in a glycine buffer, pH 8.5, containing 2-mercaptoethanol, Na_2S, and ascorbic acid.

were performed in a 40 mM glycine buffer, pH 8.5, containing Na_2S and ascorbic acid to promote reconstitution of the iron–sulfur during refolding of the protein. Nevertheless, Adx-cd was not able to reintegrate the iron–sulfur cluster, even after overnight incubation.

Interaction of Adx and Adx-cd with AdR

Using Adx-cd itself as indicator of a reduction by AdR, we could follow a reduction of Adx-cd which was reversible. However, the reaction was slow compared with the reaction between Adx and AdR, and we obtained a K_m value of 24.4 μM and a V_{max} value of 0.9 s^{-1} (Table 2).

Binding of Adx and Adx-cd to CYP11A1 and AdR

To directly test the ability of Adx-cd to bind to CYP11A1 and AdR, respectively, we performed optical biosensor studies. In measurements with different concentrations of CYP11A1, no complex formation between CYP11A1 and Adx-cd was detectable. In contrast to this result, we could observe a binding of AdR to Adx-cd.

Table 2
Parameters of Adx-cd compared to Adx

	Adx	Adx CD
Midpoint potential (mV)	-274 ± 5	-282 ± 5
T_m (oxidized form) (°C)	49.5 ± 0.3	48.7 ± 0.5
Binding to AdR, K_D (μM)	0.7 ± 0.2	4.0 ± 1.5
Binding to CYP11A1, K_D (μM)	0.13 ± 0.05	n.d.
Cholesterol side chain cleavage, K_m (μM)	0.7 ± 0.1 [10]	n.d
Cytochrome *c* reduction assay, K_m (nM)	0.3 ± 0.1 [10]	n.d
Reduction by AdR, k_{app} (max) (s^{-1})	7.3 ± 1.0 [11]	0.9430 ± 0.1

n.d., not detectable.

The binding curves were obtained using concentrations of AdR from 10 nM to 2 μM and were analyzed assuming a one-to-one interaction with a drifting baseline. The resulting K_D value was 7.7×10^{-7} M for Adx and 4.0×10^{-6} M for Adx-cd.

Reconstitution of cholesterol side-chain cleavage activity

Further, the ability of the mutant to support the conversion of cholesterol to pregnenolone was studied in a recon-

stituted system with AdR and CYP11A1. However, even with prolonged reaction time and increased amount of ferredoxin no product formation could be detected with Adx-cd.

Docking experiments

To help explain the experimental results, docking studies were carried out using the program DOT. As shown in Fig. 2, the most probable binding position of Adx-cd at the AdR surface (Fig. 2C) is not identical with the position determined for the Adx (Fig. 2A) by X-ray crystallography [5]. Two preferential binding sites exist among the 20 docking sites of lowest energy. Five of the Adx-cd models bind to the left site of the NADPH-binding cleft, namely to AdR Lys345 and AdR Glu307, and fit into the NADPH-binding cleft. The [2Fe–2S] cluster is positioned far away from the isoalloxazine of AdR. The ten lowest-energy configurations are represented by an Adx-cd molecule shown in Fig. 2B. Putatively interacting charged residues of AdR belong to two spots around Arg198, Arg234, and Arg242, and Lys369 and Arg370, respectively, and the corresponding counterparts Asp11, Glu13, Asp35 and Asp37, as well as Asp23, Asp27, and Glu43 of Adx-cd (Fig. 2D). The electron donor and acceptor are 17 Å apart, a reasonable distance for electron transfer. Only one of the docked Adx-cd molecules occupies a position similar to that within the AdR · Adx complex. Here, Lys208, Arg211, Lys243, Arg244, and Lys59 of AdR interact with Glu13, Asp35, Asp37, and Glu43 of Adx-cd (colored green in Fig. 2B). Binding of Adx-cd to P450scc was not modeled, because no structure is known for the cytochrome.

Discussion

Ferredoxins belong to a broad family of proteins present in bacteria, plants, and animals. They are divided into plant- and vertebrate-type ferredoxins, depending on their structure and function. Physiologically, ferredoxins function as one-electron carriers in a variety of redox reactions, transferring electrons to cytochromes and other proteins in subsequent steps. The tertiary structure of ferredoxins displays two main regions, an iron–sulfur cluster containing core domain and a variable interaction domain [32,33]. The larger hydrophobic core folds into a β-grasp motif which is highly conserved among ferredoxins, whereas the smaller interaction domain displays structural differences for the subfamilies.

In bovine adrenodoxin, the residues 1–55 and 91–128 belong to the core domain whereas the region between the residues 56 and 90 forms the acidic interaction domain. The [2Fe–2S] type iron–sulfur cluster is embedded into the hydrophobic core domain close to the surface of the protein and is coordinated by four cysteines (Cys46, Cys52, Cys55, and Cys92) [3,17].

Electron transfer pathway calculations using the program HARLEM revealed highest electronic coupling between the cluster iron and amino-acid residues on the surface of the core domain [10]. This indicates that electrons are most probably transferred via this region. In agreement with this, the interaction domain in adrenodoxin shows only small coupling values, indicating a low involvement of this region in direct electron transfer of ferredoxins [32].

The function of the interaction domain is rather the recognition of the redox partners and the tuning of the

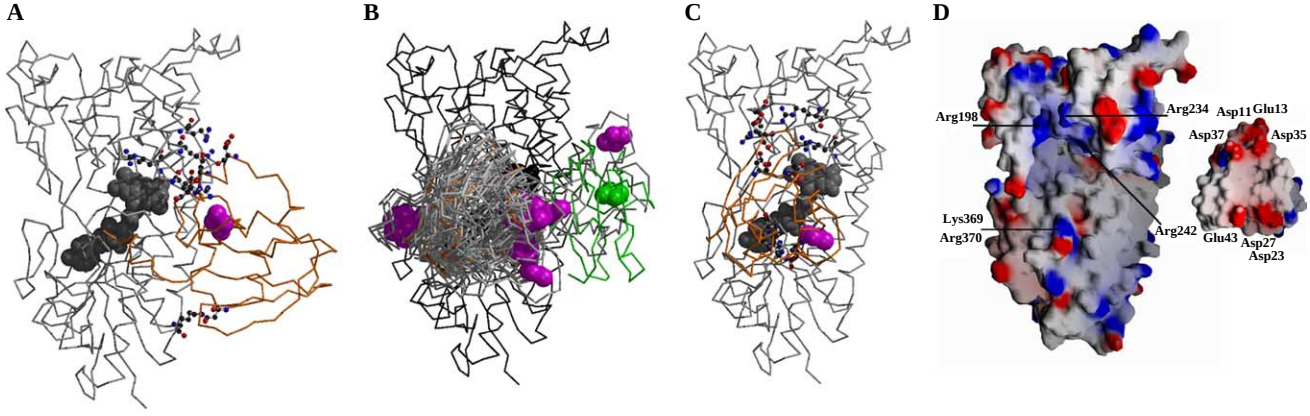

Fig. 2. Crystal structure of adrenodoxin–adrenodoxin reductase complex and complexes of Adx-cd docked to AdR by electrostatic and van der Waals energy minimization using program DOT [30]. (A) Crystal structure of the wild-type Adx · AdR complex [5]. Adx is colored orange, AdR gray, the [2Fe–2S] cluster in cpk representation magenta, FAD in cpk representation dark gray, and amino-acid side chains in the primary and secondary interaction sites [5] are shown as balls and sticks. (B) Twenty docked AdR · Adx-cd complexes of lowest energy. AdR is colored dark gray and Adx-cd light gray. The Adx-cd colored green occupies an equivalent position as the Adx in the Adx · AdR crystal structure, the Adx-cd colored orange marks the docked Adx-cd position of minimal energy. (C) Docked AdR · Adx-cd complex of lowest energy. Side chains included in the interaction are shown in ball-and-stick representation. Figure was produced with MOLSCRIPT [39]. (D) Electrostatic interactions between AdR and Adx-cd within the best-energy complex calculated by program DOT. Surface drawings of AdR (left) and Adx-cd (right). Adx-cd is rotated by 180° relative to its orientation within the complex. Surfaces are colored corresponding to the electrostatic potential for an ionic strength of 0.1 M. The deepest blue and red correspond to potentials of ± 10 kT. Blue surface regions have positive potential, and red surfaces have negative potential. Interacting amino acids are labeled. Surfaces were calculated and displayed with GRASP [40].

electron transfer complex, which is influenced by structural changes during the redox process [14,16]. Any conformational change of the iron–sulfur region can be further transferred to the flexible interaction domain via the hydrogen bond system of the crucial His56 positioned at the interface between the core domain to the interaction domain [34].

This histidine in position 56, together with 19 proximate amino acids covering the complete interaction domain, was deleted in this study resulting in the mutant protein Adx-cd. Interestingly, the recombinant protein can be expressed and purified as a stable holoprotein, which displays UV/visible spectra typical for a [2Fe–2S] cluster containing ferredoxin in the oxidized state (Fig. 1A). Slight changes in the absorption maxima indicate alterations in the environment of the cluster which could be confirmed by CD and EPR measurements (Figs. 1B and C). These results clearly show that the core domain itself is sufficient to integrate the iron–sulfur cluster as well as to fold properly in order to ensure the structural requirements for the basic functions of the ferredoxin.

Moreover, the iron–sulfur cluster has been integrated in a functional, redox-active, manner as shown by UV/visible spectra after reduction with sodium dithionite. The cluster possesses an only slightly changed redox potential compared to wild-type adrendoxin (Adx: −274 mV, Adx-cd: −282 mV). This effect on the potential turned out to be unexpectedly weak but can be explained on the one hand by an only marginal influence of the deleted 6 negative charges of the interaction domain. On the other hand, the deletion of the hydrogen bonds connecting both domains seems not to lead to a persistent distortion of the hydrogen network in the cluster vicinity. In addition, the EPR results suggest only a slight conformational change in the cluster environment, consistent with nearly unaltered accessibility to the solvent, which might lower the midpoint potential in the mutant only slightly. Taken together, the described experimental results reveal that the core domain itself is sufficient to control the redox properties of the iron–sulfur cluster of the ferredoxin, indicating that the basic structural requirements of the ferredoxin to function as an electron transporter have been maintained in the three-dimensional design of the core domain.

Furthermore, our results also indicate that the folding process of the core domain of Adx is independent from the interaction domain, which is a prerequisite for the incorporation and stability of the iron–sulfur cluster. A similar conclusion was drawn by Sow et al. [35]. Their artificial redox-active miniferredoxin, consisting of a 31 amino-acid polypeptide, could integrate a [4Fe–4S] cluster in the absence of an interaction domain and showed similar spectroscopic properties as the ferredoxin of *Desulfovibrio gigas*. The folding process of ferredoxins is driven by a multitude of hydrophobic interactions and many hydrogen bonds which stabilize the core domain. In this context, residue Pro108 plays a pivotal role for the correct folding of Adx because this amino acid has been proposed to form a hydrogen bond with residue Arg14 [36], which is essential for correct folding of the protein. This hydrogen bond, which is expected to be still present in Adx-cd, forms a connection between the carboxy and the amino terminus and stabilizes the protein. In contrast, the salt bridge between Glu74 and Arg89 seems to be dispensable for stabilizing the core domain, although it is important for the folding and stability of the full-length Adx [37]. On the other hand, removing the amino acids of the interaction domain destabilizes Adx-cd to a certain extent as indicated by thermal unfolding experiments. Nevertheless, it has to be noted that the core domain, independently of the interaction domain, is stable enough to exist as a mini-Adx.

In order to examine if Adx-cd also satisfies the other criteria of a ferredoxin, e.g., to form complexes with the redox partner proteins, optical biosensor measurements have been performed. The calculated K_D value for the binding of AdR to Adx-cd was increased by a factor of 5 compared with the interaction of AdR and Adx (Table 2), which leads to the suggestion that the complex formed is tight enough to allow an electron transfer between these proteins. The assumption that the natural electron donor AdR can reduce Adx-cd was confirmed by electron transfer assays containing NADPH, AdR, and Adx-cd. However, the rate of the Adx-cd reduction by AdR is one order of magnitude lower compared with Adx (Table 2).

This is in agreement with the electrostatic potential calculations and computer docking experiments. In the ten lowest-energy docking models, Adx-cd binds to a putative interacting site of AdR represented by two charged areas around Arg198/Arg234/Arg242 and Lys369/Arg370, respectively. The corresponding counterparts of Adx-cd are formed by the negatively charged areas Asp11/Glu13/Asp35/Asp37 and Asp23/Asp27/Glu43 (Fig. 1D). The calculated interaction site of Adx-cd with AdR is overlapping but not identical with an interaction area which has been proposed recently as second interaction region on the basis of protein–protein cross linking, crystal structure analysis, and site-directed mutagenesis studies [5,10]. The calculations indicate a distance of 17 Å between electron donor and acceptor which is reasonable for electron transfer but is about 7 Å longer than that experimentally observed in the complex of AdR with Adx. This is in agreement with a reduced rate of electron transfer from AdR to Adx-cd.

In contrast to the above results for the complex formation with AdR, no interaction between the Adx-cd mutant and CYP11A1 could be detected in biosensor measurements. This correlates with the results obtained in the CYP11A1-dependent substrate conversion assay, containing a reconstituted system with AdR, NADPH, CYP11A1, and Adx-cd. In this assay, no substrate conversion could be detected; even prolonged reaction times did not lead to product formation. The complex formation and the following electron transfer in this reaction thus appear to depend on the interaction domain of Adx. Surprisingly, in assays using cytochrome *c* as artificial electron acceptor, also no electron transfer could be detected. This suggests that Adx-cd, although being able to accept electrons from

AdR, is unable to deliver them to the cytochromes without the interaction domain. The data are also consistent with our previous results demonstrating that the interaction between Adx and AdR is only slightly ionic-strength-dependent, whereas the interaction of Adx and CYP11A1 shows a clear salt effect [38].

In this context, it has to be mentioned that the interaction domains of ferredoxins show significant structural differences between the subfamilies, whereas their core domains are highly conserved. The structural differences and therefore the importance of the interaction domains for the binding of the redox partner cytochrome P450 can be explained by a co-evolution of interaction domain and cytochrome P450, a process which was driven by a constantly increasing number of cytochromes P450 [1]. In contrast to this, the number of reductase isoforms remained constant [6]. As a consequence, the residual surface of the core domain conserved all basic characteristics needed for the interaction with AdR, a process optimized early in molecular evolution, but is lacking essential characteristics for the binding to CYP11A1, which might have been established evolutionarily later.

Summarizing, we demonstrate the construction and purification of an adrenodoxin mutant, Adx-cd, possessing only the iron–sulfur cluster containing core domain but missing the whole interaction domain. Although numerous residues have been deleted, the core domain restored all structural information for a proper folding and integration of a prosthetic group. Adx-cd may thus be reminiscent of an archetypical redox-active ferredoxin, which can functionally bind to its electron donor but has not yet gained the capacity to interact with its electron acceptor which arrived later in molecular evolution.

Acknowledgments

We thank Wolfgang Reinle and Walter Klose for purifying AdR and CYP11A1 and Dr. Reinhold Kappl for EPR measurements.

References

[1] R. Bernhardt, Cytochrome P450: structure, function, and generation of reactive oxygen species, Rev. Physiol. Biochem. Pharmacol. 127 (1996) 137–221.
[2] H. Uhlmann, V. Beckert, D. Schwarz, R. Bernhardt, Expression of bovine adrenodoxin in *E. coli* and site-directed mutagenesis of /2 Fe-2S/ cluster ligands, Biochem. Biophys. Res. Commun. 188 (1992) 1131–1138.
[3] A. Müller, J.J. Müller, Y.A. Müller, H. Uhlmann, R. Bernhardt, U. Heinemann, New aspects of electron transfer revealed by the crystal structure of a truncated bovine adrenodoxin, Adx(4-108), Structure 6 (1998) 269–280.
[4] E.-C. Müller, A. Lapko, A. Otto, J.J. Müller, K. Ruckpaul, U. Heinemann, Covalently crosslinked complexes of bovine adrenodoxin with adrenodoxin reductase and cytochrome P450scc: mass spectrometry and Edman degradation of complexes of the steroidogenic hydroxylase system, Eur. J. Biochem. 268 (2001) 1837–1843.
[5] J.J. Müller, A. Lapko, G. Bourenkov, K. Ruckpaul, U. Heinemann, Adrenodoxin reductase-adrenodoxin complex structure suggests electron transfer path in steroid biosynthesis, J. Biol. Chem. 276 (2001) 2786–2789.
[6] L.E. Vickery, Molecular recognition and electron transfer in mitochondrial steroid hydroxylase systems, Steroids 62 (1997) 124–127.
[7] J.A. Harikrishna, S.M. Black, G.D. Szklarz, W.L. Miller, Construction and function of fusion enzymes of the human cytochrome P450scc system, DNA Cell. Biol. 12 (1993) 371–379.
[8] V.M. Coghlan, L.E. Vickery, Site-specific mutations in human ferredoxin that affect binding to ferredoxin reductase and cytochrome P450scc, J. Biol. Chem. 266 (1991) 18606–18612.
[9] V. Beckert, R. Dettmer, R. Bernhardt, Mutations of tyrosine 82 in bovine adrenodoxin that affect binding to cytochromes P45011A1 and P45011B1 but not electron transfer, J. Biol. Chem. 269 (1994) 2568–2573.
[10] F. Hannemann, M. Rottmann, B. Schiffler, J. Zapp, R. Bernhardt, The loop region covering the iron–sulfur cluster in bovine adrenodoxin comprises a new interaction site for redox partners, J. Biol. Chem. 276 (2001) 1369–1375.
[11] A. Zöllner, F. Hannemann, M. Lisurek, R. Bernhardt, Deletions in the loop surrounding the iron–sulfur cluster of adrenodoxin severely affect the interactions with its native redox partners adrenodoxin reductase and cytochrome P450(scc) (CYP11A1), J. Inorg. Biochem. 91 (2002) 644–654.
[12] B. Schiffler, M. Kiefer, A. Wilken, F. Hannemann, H.W. Adolph, R. Bernhardt, The interaction of bovine adrenodoxin with CYP11A1 (cytochrome P450scc) and CYP11B1 (cytochrome P45011b): acceleration of reduction and substrate conversion by site-directed mutagenesis of adrenodoxin, J. Biol. Chem. 276 (2001) 36225–36232.
[13] T. Kido, T. Kimura, The formation of binary and ternary complexes of cytochrome P-450scc with adrenodoxin and adrenodoxin reductase.adrenodoxin complex. The implication in ACTH function, J. Biol. Chem. 254 (1979) 11806–11815.
[14] J.D. Lambeth, D.W. Seybert, H. Kamin, Ionic effects on adrenal steroidogenic electron transport. The role of adrenodoxin as an electron shuttle, J. Biol. Chem. 254 (1979) 7255–7264.
[15] M. Takeshima, T. Hara, High density lipoprotein cholesterol as a mechanistic probe for the side chain cleavage reaction, Biochem. Biophys. Res. Commun. 179 (1991) 161–169.
[16] D. Beilke, R. Weiss, F. Lohr, P. Pristovsek, F. Hannemann, R. Bernhardt, H. Rüterjans, A new electron transport mechanism in mitochondrial steroid hydroxylase systems based on structural changes upon the reduction of adrenodoxin, Biochemistry 41 (2002) 7969–7978.
[17] I.A. Pikuleva, K. Tesh, M.R. Waterman, Y. Kim, The tertiary structure of full-length bovine adrenodoxin suggests functional dimers, Arch. Biochem. Biophys. 373 (2000) 44–55.
[18] F.W. Studier, B.A. Moffatt, Use of bacteriophage T7 RNA polymerase to direct selective high-level expression of cloned genes, J. Mol. Biol. 189 (1986) 113–130.
[19] Y. Sagara, A. Wada, Y. Takata, M.R. Waterman, K. Sekimizu, T. Horiuchi, Direct expression of adrenodoxin reductase in *Escherichia coli* and the functional characterization, Biol. Pharm. Bull. 16 (1993) 627–630.
[20] T. Kimura, in: C.K. Jorgensen, J.B. Neilands, R.S. Nyholm, D. Reinen, R.J.P. Williams (Eds.), Structure and Bonding, Springer-Verlag, Berlin, 1968, pp. 1–40.
[21] A. Hiwatashi, Y. Ichikawa, T. Yamano, N. Maruya, Properties of crystalline reduced nicotinamide adenine dinucleotide phosphate-adrenodoxin reductase from bovine adrenocortical mitochondria. II. Essential histidyl and cysteinyl residues at the NADPH binding site of NADPH-adrenodoxin reductase, Biochemistry 15 (1976) 3091–3097.
[22] A.A. Akhrem, V.N. Lapko, A.G. Lapko, V.M. Shkumatov, V.L. Chashchin, Isolation, structural organization and mechanism of action of mitochondrial steroid hydroxylating systems, Acta Biol. Med. Ger. 38 (1979) 257–273.
[23] H. Uhlmann, R. Kraft, R. Bernhardt, C-terminal region of adrenodoxin affects its structural integrity and determines differences in its electron transfer function to cytochrome P-450, J. Biol. Chem. 269 (1994) 22557–22564.

[24] P.L. Privalov, Stability of proteins: small globular proteins, Adv. Protein Chem. 33 (1979) 167–241.
[25] A. Fersht, Protein stability, in: M.R. Julet (Ed.), Structure and Mechanism in Protein Science, Freeman, W.H. and Company, 1999, pp. 508–539.
[26] S.G. Sligar, I.C. Gunsalus, A thermodynamic model of regulation: modulation of redox equilibria in camphor monoxygenase, Proc. Natl. Acad. Sci. USA 73 (1976) 1078–1082.
[27] S. Sugano, R. Miura, N. Morishima, Identification of intermediates in the conversion of cholesterol to pregnenolone with a reconstituted cytochrome p-450scc system: accumulation of the intermediate modulated by the adrenodoxin level, J. Biochem. (Tokyo) 120 (1996) 780–787.
[28] T. Schwede, J. Kopp, N. Guex, M.C. Peitsch, SWISS-MODEL: an automated protein homology-modeling server, Nucleic Acids Res. 31 (2003) 3381–3385.
[29] J.J. Müller, A. Lapko, K. Ruckpaul, U. Heinemann, Modeling of electrostatic recognition processes in the mammalian mitochondrial steroid hydroxylase system, Biophys. Chem. 100 (2003) 281–292.
[30] L.F. Ten Eyck, J. Mandrell, V.A. Roberts, M.E. Pique, in: Supercomputing 95, IEEE Computer Society Press, Los Alamitos, CA, 1995, p. 12.
[31] D.A. Pearlman, D.A. Case, J.W. Caldwell, W.S. Ross, T.E. Cheatham, S. DeBolt, D. Ferguson, G. Seibel, P. Kollman, AMBER, a package of computer programs for applying molecular mechanics, normal mode analysis, molecular dynamics and free energy calculations to simulate the structural and energetic properties of molecules, Comp. Phys. Commun. 91 (1995) 1–41.
[32] J.J. Müller, A. Müller, M. Rottmann, R. Bernhardt, U. Heinemann, Vertebrate-type and plant-type ferredoxins: crystal structure comparison and electron transfer pathway modelling, J. Mol. Biol. 294 (1999) 501–513.
[33] S.C. Im, G. Liu, C. Luchinat, A.G. Sykes, I. Bertini, The solution structure of parsley [2Fe–2S]ferredoxin, Eur. J. Biochem. 258 (1998) 465–477.
[34] V. Beckert, H. Schrauber, R. Bernhardt, A.A. Van Dijk, C. Kakoschke, V. Wray, Mutational effects on the spectroscopic properties and biological activities of oxidized bovine adrenodoxin, and their structural implications, Eur. J. Biochem. 231 (1995) 226–235.
[35] T.C. Sow, M.V. Pederson, H.E. Christensen, B.L. Ooi, Total synthesis of a miniferredoxin, Biochem. Biophys. Res. Commun. 223 (1996) 360–364.
[36] A. Grinberg, R. Bernhardt, Structural and functional consequences of substitutions at the Pro108-Arg14 hydrogen bond in bovine adrenodoxin, Biochem. Biophys. Res. Commun. 249 (1998) 933–937.
[37] A.V. Grinberg, R. Bernhardt, Contribution of a salt bridge to the thermostability of adrenodoxin determined by site-directed mutagenesis, Arch. Biochem. Biophys. 396 (2001) 25–34.
[38] B. Schiffler, A. Zöllner, R. Bernhardt, Stripping down the mitochondrial cholesterol hydroxylase system, a kinetics study, J. Biol. Chem. 279 (2004) 34269–34276.
[39] P.J. Kraulis, MOLSCRIPT: a program to produce both detailed and schematic plots of protein structures, J. Appl. Crystallogr. 24 (1991) 946–950.
[40] A. Nicholls, K.A. Sharp, B. Honig, Protein folding and association: insights from the interfacial and thermodynamic properties of hydrocarbons, Proteins 11 (1991) 281–296.